

Optimized Energy and Information Relaying in Self-Sustainable IRS-Empowered WPCN

Bin Lyu, Parisa Ramezani, Dinh Thai Hoang, Shimin Gong, Zhen Yang, and Abbas
Jamalipour

Abstract

This paper proposes a hybrid-relaying scheme empowered by a self-sustainable intelligent reflecting surface (IRS) in a wireless powered communication network (WPCN), to simultaneously improve the performance of down-link energy transfer (ET) from a hybrid access point (HAP) to multiple users and uplink information transmission (IT) from users to the HAP. We propose time-switching (TS) and power-splitting (PS) schemes for the IRS, where the IRS can harvest energy from the HAP's signals by switching between energy harvesting and signal reflection in the TS scheme or adjusting its reflection amplitude in the PS scheme. For both the TS and PS schemes, we formulate the sum-rate maximization problems by jointly optimizing the IRS's phase shifts for both ET and IT and network resource allocation. To address each problem's non-convexity, we propose a two-step algorithm, where the formulated problem is decoupled into two sub-problems and each sub-problem can be solved separately in an efficient way. To show the structure of resource allocation, we also investigate sub-optimal solutions for the schemes with random phase shifts. Through numerical results, we show that our proposed schemes can achieve over hundred times sum-rate gain compared to the baseline scheme without IRS.

Index Terms

Wireless powered communication network, intelligent reflecting surface, time scheduling, phase shift optimization.

B. Lyu and Z. Yang are with Key Laboratory of Ministry of Education in Broadband Wireless Communication and Sensor Network Technology, Nanjing University of Posts and Telecommunications, Nanjing 210003, China (email: blyu@njupt.edu.cn, yangz@njupt.edu.cn).

P. Ramezani and A. Jamalipour are with School of Electrical and Information Engineering, University of Sydney, Sydney, NSW 2006, Australia (email: parisa.ramezani@sydney.edu.au, a.jamalipour@ieee.org)

D. T. Hoang is with School of Electrical and Data Engineering, University of Technology Sydney, Sydney, NSW 2007, Australia (email: hoang.dinh@uts.edu.au).

S. Gong is with School of Intelligent Systems Engineering, Sun Yat-sen University, Guangzhou 510275, China (email: gong-shm5@mail.sysu.edu.cn).

I. INTRODUCTION

With nearly 50 billion Internet of Things (IoT) devices by 2020 and even 500 billion by 2030 [1], we have already stepped into the new era of IoT. Having the vision of being self-sustainable, IoT has observed the energy limitation as a major issue for its widespread development. Recent advances in energy harvesting (EH) technologies, especially radio frequency (RF) EH [2], opened a new approach for self-sustainable IoT devices to harvest energy from dedicated or ambient RF sources. This leads to an emerging topic of wireless powered communication networks (WPCNs), in which low-cost IoT devices can harvest energy from a dedicated hybrid access point (HAP) and then use the harvested energy to transmit data to the HAP [3]. As a result, the development of WPCNs has been a promising step toward the future self-sustainable IoT networks [4].

Although possessing significant benefits and attractive features for low-cost IoT networks, e.g., multi-device and long-distance charging, WPCNs are facing some challenges which need to be addressed before they can be widely deployed in practice. In particular, the uplink information transmission (IT) of IoT devices in WPCNs relies on their harvested energy from downlink energy transfer (ET) of the HAP. However, the IoT devices typically suffer from doubly attenuations of RF signal power over distance [3], which severely limits the network performance, e.g., the amount of energy harvested by the IoT devices and achievable rates at the HAP. Hence, solutions to enhance the downlink ET efficiency and improve the uplink transmission rates for WPCNs are urgent needs. Reducing the distances between the HAP and IoT devices is one solution to enhance EH efficiency and achieve greater transmission rates. However, this is not a viable option because IoT devices are randomly deployed in practice, and thus we may not be able to control all of them over their locations. Hence, more efficient and cost-effective solutions are required to guarantee that WPCN can be seamlessly fitted into the IoT environment with satisfying performance.

Relay cooperation is an efficient way to enhance the performances of WPCNs, which can be classified into two categories of active relaying and passive relaying. Active relaying refers to scenarios in which the communication between a transmitter and its destined receiver is assisted by a relay which forwards the users information to the destination via active RF transmission [5]-[7]. However, active relaying schemes have several limitations. Considering that the relays are energy-constrained, they need to harvest sufficient energy from the RF sources and use the harvested energy to actively forward information to the receiver. Due to the higher circuit power consumption of active relays, it may take long for these relay to harvest enough energy. This reduces the IT time of the network. Besides, most active relays operate in half-duplex

mode, which further shortens the effective IT time, resulting in network performance degradation. Full-duplex (FD) relays can relax this issue; however, complex self-interference (SI) cancellation techniques are needed at FD relays to ensure that SI is effectively mitigated [8].

Passive relaying exploits the idea of backscatter communication (BackCom) for assisting the source-destination communication [9]-[11]. Specifically, BackCom relay nodes do not need any RF components as they passively backscatter the sources signal to strengthen the received signal at the receiver. Accordingly, the power consumption of BackCom relay nodes is extremely low and no dedicated time is needed for the relays EH [12]. Nonetheless, as no active signal generation is involved and the passive relays simply reflect the received signal from the source, passive relaying schemes suffer from poor performance.

Intelligent reflecting surface (IRS), consisting of a large number of low-cost reflecting elements, has recently emerged as a promising solution to improve the performance of wireless communication networks [13], [14]. IRS elements smartly induce phase shifts and amplitude change to the incident signals and passively reflect them such that the signals are constructively combined at the receiver. In this way, IRS can adjust the communication environment and create favorable conditions for energy and information transmission without using energy-hungry RF chains. This technology has lately been utilized for total transmit power minimization in wireless communication networks [15], ET enhancement in multiple-input single-output (MISO) systems [16], weighted sum-power and weighted sum-rate maximization in simultaneous wireless information and power transfer (SWIPT) systems [17], [18], spectrum efficiency maximization in MISO communication systems [19], secure transmit power allocation [20], outage probability minimization [21], etc., and demonstrated promising results and significant performance gains as compared to the conventional wireless networks without IRS.

Having the capability of cooperating in downlink ET and uplink IT, IRS has several advantages over the conventional active and passive relaying techniques [13]. First of all, IRS is a cost-effective technology and it can be readily integrated into existing wireless communication networks without incurring high implementation costs. Furthermore, IRS is more energy- and spectrum-efficient as compared to conventional relaying methods because it consumes very low power and at the same time, helps using the limited spectrum resources more efficiently. IRS essentially works in the full-duplex mode without causing any interference and adding thermal noise, which further improves the spectral efficiency. Moreover, it is easy to increase the number of IRS elements to achieve higher performance gains. Motivated by its numerous benefits, IRS offers a promising green solution to improve the performance for WPCNs. Recently, a few

research works have investigated the application of IRS for improving the performance of WPCNs [22], [23]. In our preliminary work [22], we proposed a solution using the IRS as a hybrid relay to simultaneously improve energy and data communications efficiency for WPCNs, where the IRS first operates as an energy relay to assist the downlink ET from the HAP to a number of users and then works as an information relay to help the uplink IT from the users to the HAP. Zheng *et al.* proposed a similar idea to use the IRS as a hybrid relay, which is not only used to enhance both ET and IT efficiency but also involved in user cooperation [23]. However, [23] only considered a two-user scenario and the proposed solution is not applicable to the general scenario with multiple users. More importantly, [15]-[23] assume that the energy consumption of IRS is negligible because it does not need any active RF chains but only reflects incident signals passively. However, as mentioned in [24]-[26], the energy consumption of IRS is in fact proportional to the number of IRS elements. Hence, the energy consumption of IRS cannot be ignored since the number of IRS elements is relatively large to achieve better performance. Thus, it is challenging to power IRS and keep its hybrid-relaying operations in WPCNs.

To address the above issue effectively, we propose a self-sustainable IRS-empowered WPCN, where the IRS is equipped with EH circuit to harvest RF energy from the HAP to power its operations. Similar to the conventional wireless-powered active relays [27], time-switching (TS) and power-splitting (PS) schemes are proposed to enable IRS to harvest energy from the RF signals transmitted by the HAP. In the TS scheme, the ET phase is split into two sub-slots, where the IRS harvests energy in the first sub-slot and assists in downlink ET to the users in the second sub-slot. In the PS scheme, the IRS harvests energy from the HAP's signal by adjusting its amplitude reflection coefficients. To maximize the system sum-rate for both TS and PS schemes, we thus need to optimize IRS phase shift design and network resource allocation jointly with EH time and amplitude reflection coefficients of the IRS. This optimization is thus much more challenging to address than the ones studied in other works on IRS and conventional wireless-powered relays. Therefore, we propose efficient algorithms to find the optimal solutions to the sum-rate maximization problems for both TS and PS schemes. Numerical simulations endorse the effectiveness of our proposed schemes for improving the performance of WPCN and show remarkable performance gain as compared to the baseline WPCN without IRS in [3].

The main contributions of this paper are summarized as follows:

- We propose a self-sustainable IRS-empowered WPCN, where a wireless-powered IRS acts as a hybrid relay to improve the performance of WPCN in both downlink ET from the HAP to the users and

uplink IT from users to the HAP.

- To enable energy collection and hybrid relaying functionalities at the IRS, we consider TS and PS schemes, where the IRS uses a portion of the ET phase for its own EH in the TS scheme or adjusts its amplitude reflection coefficients to harvest energy from a part of the received energy signal in the PS scheme.
- We study the system sum-rate maximization problem for the TS scheme by jointly optimizing the IRS's phase shift design in both ET and IT phase, time allocation for the IRS and users' EH, time allocation for each user' IT, and the users' power allocation. To deal with the non-convexity of the formulated problem, we propose a two-step algorithm, where the problem is decoupled into two sub-problems. For the first sub-problem, showing that the optimal phase shift design in the IT phase is independent of other variables, we find the optimal phase shifts at the IRS in each time-slot of the IT phase by applying the semidefinite relaxation (SDR) [28] and Gaussian randomization methods. We then solve the second sub-problem to find the optimal values of other optimization variables. In particular, we obtain the IRS's EH time in a closed-form and discuss its implications. We finally obtain the optimal solution to our problem by sequentially solving the two sub-problems.
- We then investigate the sum-rate maximization problem for the PS scheme and jointly optimize the IRS's phase shift design in both ET and IT phase, time allocation for the EH and IT phases, power allocation at the users, and the amplitude reflection coefficients in the EH phase, using a similar two-step algorithm as for the TS scheme. We obtain the optimal amplitude reflection coefficient as a function of the EH time, from which some interesting observations are revealed.
- To shed more light on the structure of resource allocation for our proposed schemes, we also investigate special problems of optimizing time and power allocation with random phase shifts for both TS and PS schemes.
- Finally, we evaluate the performance of our proposed schemes via numerical results, which show that our proposed schemes can achieve over *hundred times* sum-rate gain as compared to the baseline WPCN protocol in [3]. In addition, we show that the PS scheme usually achieves a better performance than the TS scheme. However, the PS scheme is not applicable when the HAP's transmit power is low and/or the channel between the HAP and IRS is weak.

This paper is organized as follows. Section II describes the system model of the proposed IRS-assisted WPCN for both TS and PS methods. Sections III and IV investigate the sum-rate maximization problems

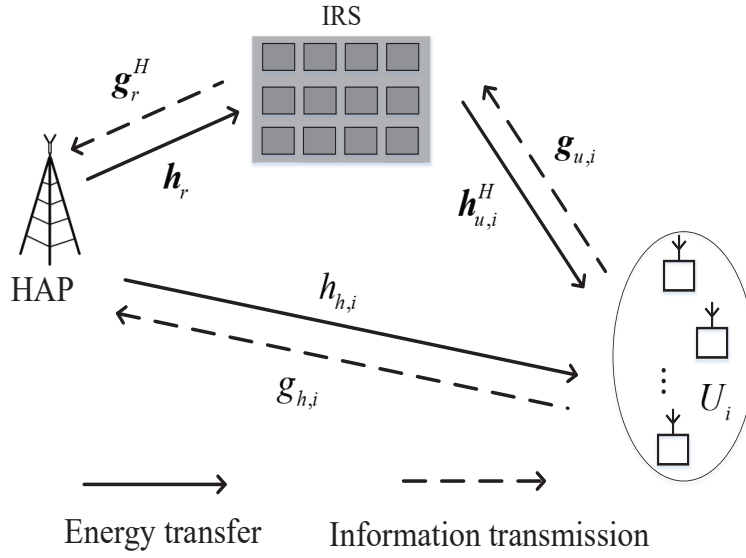


Fig. 1. System model for an IRS-assisted WPCN.

for TS and PS methods, respectively. Section V evaluates the performance of the presented algorithms by conducting numerical simulations and Section VI concludes the paper.

II. SYSTEM MODEL

As illustrated in Fig. 1, we consider an IRS-assisted WPCN, consisting of an HAP with stable power supply, N energy-constrained users (denoted by U_i , $i = 1, \dots, N$), and an energy-constrained IRS. HAP and users have single antenna each. The IRS is composed of K passive reflecting elements, which can be configured to direct the incident signals to desired directions. The IRS assists in both downlink ET from the HAP to the users and uplink IT from the users to the HAP.

The downlink channels from the HAP to U_i , from the HAP to the IRS, and from the IRS to U_i are denoted by $\mathbf{h}_{h,i}$, $\mathbf{h}_r \in \mathcal{C}^{K \times 1}$, and $\mathbf{h}_{u,i}^H \in \mathcal{C}^{1 \times K}$, respectively. The counterpart uplink channels are denoted by $\mathbf{g}_{h,i}$, $\mathbf{g}_r^H \in \mathcal{C}^{1 \times K}$, and $\mathbf{g}_{u,i} \in \mathcal{C}^{K \times 1}$, respectively. All channels are assumed to be quasi-static flat fading, which remain constant during one block but may change from one block to another [17]. We assume that the channel state information (CSI) of all links is perfectly known¹.

The transmission block, normalized to one, is divided into two phases, i.e., ET phase and IT phase. In the ET phase, the HAP transfers energy to the users and IRS in the downlink. The IRS uses the harvested energy from HAP's signals for its own EH and energy relaying to the users. In the IT phase, the users

¹The CSI of all links can be precisely estimated by the advanced channel estimation techniques. Even if there exist channel estimation errors in realistic scenarios, the sum-rate derived under the perfect CSI condition can serve as an upper-bound for the system performance.

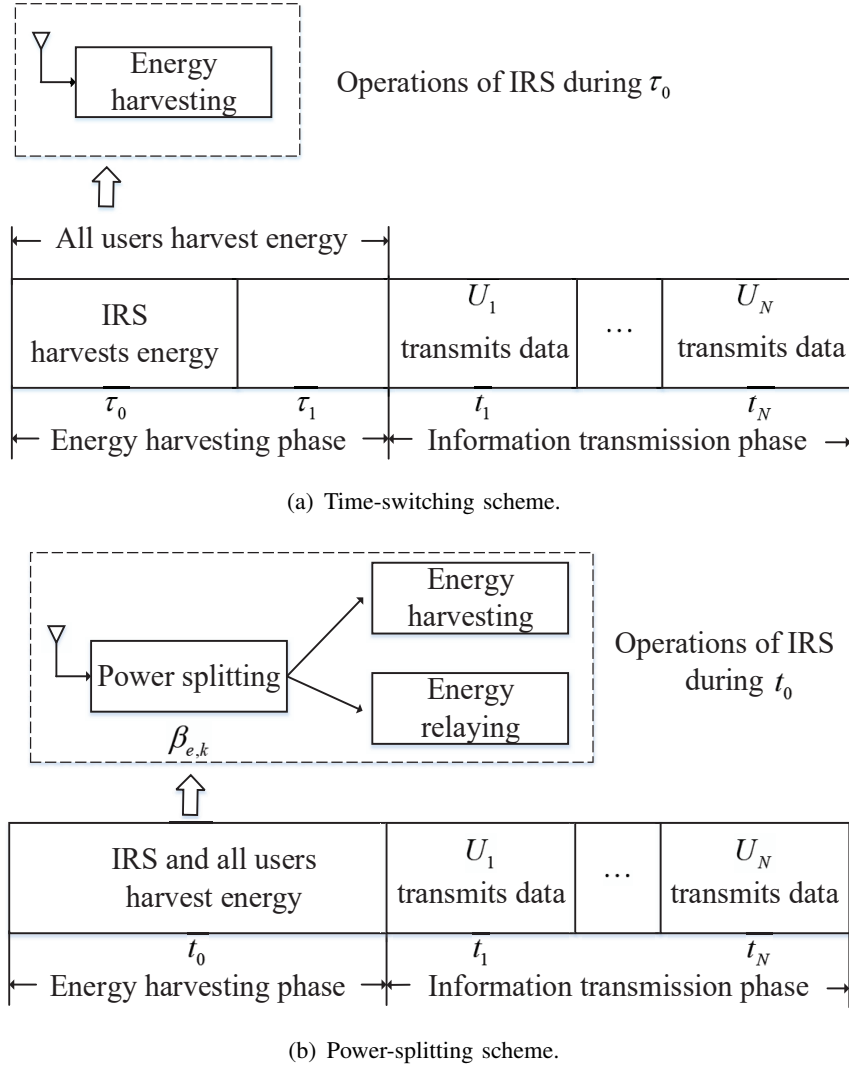


Fig. 2. Transmission block structure.

use the harvested energy to transmit data to the HAP with the assistance of the IRS. The details of the ET and IT phases are shown in Fig. 2 and elaborated in the following subsections.

A. Energy Transfer Phase

As mentioned earlier, the IRS is assumed to be energy-constrained, which needs to harvest energy from the HAP for powering its relaying operations. In this regard, we consider TS and PS schemes which have been widely used in conventional wireless-powered relay communications [27].

1) *Time-switching scheme*: For the TS scheme, the ET phase with the duration of t_0 is divided into two sub-slots, having the duration of τ_0 and τ_1 , respectively, which satisfy $\tau_0 + \tau_1 \leq t_0$. In this scheme, the users can harvest energy over the entire ET phase. For the IRS, it will spend the first sub-slot in the ET phase for harvesting energy and the second sub-slot for improving the EH efficiency at the users. In

particular, in the second sub-slot, the IRS can cooperate with the HAP by adjusting its elements' phase shifts in order to enhance the total received signal power at the users. The transmission block structure for the TS scheme is illustrated in Fig. 2 (a). Denote the transmit signal in the ET phase as

$$x_h = \sqrt{P_h} s_h, \quad (1)$$

where P_h is the transmit power and s_h is the energy-carrying signal with $s_h \sim \mathcal{CN}(0, 1)$.

The received signals at the IRS and U_i in the first sub-slot are expressed as

$$\mathbf{y}_{r,0} = \mathbf{h}_r x_h + \mathbf{n}_r, \quad (2)$$

$$y_{ts,0,i} = h_{h,i} x_h + n_{u,i}, \quad i = 1, \dots, N, \quad (3)$$

where \mathbf{n}_r and $n_{u,i}$ denote the additive white Gaussian noises (AWGNs) at the IRS and U_i , respectively. Note that the noise power is usually very small and ineffective for EH and can be thus neglected. Hence, the harvested energy by the IRS, denoted by $E_{ts,r}$, is expressed as

$$E_{ts,r} = \eta P_h \|\mathbf{h}_r\|^2 \tau_0. \quad (4)$$

In the second sub-slot, the IRS assists in the downlink ET. The phase shift matrix of the IRS during τ_1 is denoted by $\Theta_e = \text{diag}\{\beta_{e,1} e^{j\theta_{e,1}}, \dots, \beta_{e,K} e^{j\theta_{e,K}}\}$, where $\beta_{e,k} \in [0, 1]$ and $\theta_{e,k} \in [0, 2\pi]$ are the amplitude reflection coefficient and the phase shift of the k -th element, respectively. For the TS scheme, since the IRS only harvests energy during τ_0 , all incident signals at the IRS during τ_1 can be reflected to enhance the EH efficiency, i.e., $\beta_{e,k} = 1, \forall k$ [13]. Let $\bar{\Theta}_e = \text{diag}\{e^{j\theta_{e,1}}, \dots, e^{j\theta_{e,K}}\}$. During τ_1 , the received signal at U_i for the TS scheme is given by

$$y_{ts,i} = (\mathbf{h}_{u,i}^H \bar{\Theta}_e \mathbf{h}_r + h_{h,i}) x_h + n_{u,i}, \quad i = 1, \dots, N. \quad (5)$$

The harvested energy of U_i for the TS scheme, denoted by $E_{ts,i}$, is thus obtained as

$$E_{ts,i} = \eta P_h |h_{h,i}|^2 \tau_0 + \eta P_h |\mathbf{h}_{u,i}^H \bar{\Theta}_e \mathbf{h}_r + h_{h,i}|^2 \tau_1, \quad (6)$$

where the first term denotes the energy harvested by U_i from the HAP directly during τ_0 , and the second term is the harvested energy with the aid of the IRS during τ_1 .

2) *Power-splitting scheme*: Different from the TS scheme, the dedicated EH time is not required in the PS scheme and the IRS harvests energy from the HAP by adjusting the amplitude reflection coefficients $(\beta_{e,k}, \forall k)$, as illustrated in Fig. 2 (b). To be specific, only a part of the HAP's energy signals is reflected by the IRS and the remaining part is fed into the IRS's EH unit for harvesting.

It is assumed that all the amplitude reflection coefficients of the IRS elements have the same value, i.e. $\beta_{e,k} = \beta_e, \forall k$, which is a reasonable assumption for simplifying the circuit design and reducing the circuit power consumption of the IRS. The received signal at U_i in the ET phase for the PS scheme is thus given by

$$y_{ps,i} = (\mathbf{h}_{u,i}^H \beta_e \bar{\Theta}_e \mathbf{h}_r + h_{h,i})x_h + n_{u,i}, \quad i = 1, \dots, N, \quad (7)$$

The harvested energy of the IRS and U_i for the PS scheme are denoted as $E_{ps,r}$ and $E_{ps,i}$, which are respectively given by

$$E_{ps,r} = \eta P_h (1 - \beta_e^2) \|\mathbf{h}_r\|^2 t_0, \quad (8)$$

$$E_{ps,i} = \eta P_h |\mathbf{h}_{u,i}^H \beta_e \bar{\Theta}_e \mathbf{h}_r + h_{h,i}|^2 t_0. \quad (9)$$

B. Information Transmission Phase

In the IT phase, the users transmit information to the HAP via time division multiple access, using the harvested energy in the ET phase. Denote the duration of IT for U_i as t_i . Let $s_{u,i}$ be the information-carrying signal of U_i with unit power. The transmit signal of U_i during t_i is then expressed as

$$x_{u,i} = \sqrt{P_{u,i}} s_{u,i}, \quad (10)$$

where $P_{u,i}$ is U_i 's transmit power and satisfies

$$P_{u,i} t_i + P_{c,i} t_i \leq E_{f,i}, \quad f = \{ts, ps\}, \quad (11)$$

with $P_{c,i}$ being the circuit power consumption of U_i . The circuit power consumption of the IRS is given by $K\mu$, where μ denotes the circuit power consumption of each reflecting element [24]-[26]. To power its operations, IRS needs to harvest sufficient energy in the ET phase. Therefore, the following constraints

are hold

$$K\mu(\tau_1 + \sum_{i=1}^N t_i) \leq E_{ts,r}, \quad (12)$$

$$K\mu(t_0 + \sum_{i=1}^N t_i) \leq E_{ps,r}, \quad (13)$$

for TS and PS schemes, respectively. Note that in the first sub-slot of the TS scheme, it is not necessary to adjust the IRS's phase shifts to reflect signals and its circuit power consumption for only EH during τ_0 is thus negligible [25].

Denote the phase shift matrix during t_i for the IT as $\Theta_{d,i}$, where $\Theta_{d,i} = \text{diag}\{e^{j\theta_{d,i,1}}, \dots, e^{j\theta_{d,i,K}}\}$. Note that we have set the amplitude reflection coefficients to be 1 to maximize the signal reflection in the IT phase. The received signal at the HAP from U_i , denoted by $y_{h,i}$, is thus given by

$$y_{h,i} = (\mathbf{g}_r^H \Theta_{d,i} \mathbf{g}_{u,i} + g_{h,i}) \sqrt{P_{u,i} s_{u,i}} + n_h, \quad (14)$$

where $n_h \sim \mathcal{CN}(0, \sigma_h^2)$ is the AWGN at the HAP. The signal-noise-ratio (SNR) at the HAP during t_i , denoted by γ_i , is expressed as

$$\gamma_i = \frac{P_{u,i} |\mathbf{g}_r^H \Theta_{d,i} \mathbf{g}_{u,i} + g_{h,i}|^2}{\sigma_h^2}. \quad (15)$$

The achievable rate from U_i to the HAP is then formulated as

$$R_i = t_i \log_2 \left(1 + \frac{P_{u,i} |\mathbf{g}_r^H \Theta_{d,i} \mathbf{g}_{u,i} + g_{h,i}|^2}{\sigma_h^2} \right). \quad (16)$$

III. SUM-RATE MAXIMIZATION FOR THE TS SCHEME

In this section, we aim to maximize the system sum-rate by jointly optimizing the phase shift design at the IRS in both ET and IT phases, time scheduling of the network for ET and IT, and power allocation

at the users. The optimization problem is formulated as

$$\begin{aligned}
& \max_{\boldsymbol{\theta}_e, \{\boldsymbol{\theta}_{d,i}\}_{i=1}^N, \mathbf{t}, \boldsymbol{\tau}, \mathbf{P}_u} \sum_{i=1}^N R_i, \\
& \text{s.t.} \quad \text{C1: } K\mu(\tau_1 + \sum_{i=1}^N t_i) \leq E_{ts,r}, \\
& \quad \text{C2: } P_{u,i}t_i + P_{c,i}t_i \leq E_{ts,i}, \quad \forall i, \\
& \quad \text{C3: } \tau_0 + \tau_1 \leq t_0, \\
& \quad \text{C4: } \sum_{i=0}^N t_i \leq 1, \\
& \quad \text{C5: } \tau_0, \tau_1 \geq 0, \\
& \quad \text{C6: } t_i \geq 0, \quad \forall i, \\
& \quad \text{C7: } P_{u,i} \geq 0, \quad \forall i, \\
& \quad \text{C8: } 0 \leq \theta_{e,k} \leq 2\pi, \quad \forall k, \\
& \quad \text{C9: } 0 \leq \theta_{d,i,k} \leq 2\pi, \quad \forall i, \quad \forall k,
\end{aligned} \tag{P1}$$

where $\mathbf{t} = [t_0, t_1, \dots, t_N]$, $\boldsymbol{\tau} = [\tau_0, \tau_1]$, $\boldsymbol{\theta}_e = [\theta_{e,1}, \dots, \theta_{e,K}]$, $\boldsymbol{\theta}_{d,i} = [\theta_{d,i,1}, \dots, \theta_{d,i,K}]$, and $\mathbf{P}_u = [P_{u,1}, \dots, P_{u,N}]$.

A. Optimal Solution to P1

It is obvious that P1 is a non-convex optimization problem due to the coupling of variables in the objective function and the constraints. In the following, we propose a two-step solution to solve the sum-rate maximization problem in P1. Specifically, we split P1 into two decoupled sub-problems, and solve each sub-problem separately.

1) *Optimizing the phase shift design for IT:* We first present a proposition for the optimal design of phase shifts of the IRS for the IT.

Lemma 1. *The optimal IRS phase shifts for the IT during t_i ($i = 1, \dots, N$) can be found by solving the following problem*

$$\begin{aligned}
& \boldsymbol{\theta}_{d,i}^* = \arg \max_{\boldsymbol{\theta}_{d,i}} |\mathbf{g}_r^H \boldsymbol{\Theta}_{d,i} \mathbf{g}_{u,i} + g_{h,i}|^2, \\
& \text{s.t. } 0 \leq \theta_{d,i,k} \leq 2\pi, \quad \forall k.
\end{aligned} \tag{P2}$$

Proof. Refer to Appendix A. □

According to Lemma 1, we proceed to solve **P2** to obtain the optimal phase shifts for the IT. Denote $v_{d,i,k} = e^{j\theta_{d,i,k}}$, where $|v_{d,i,k}| = 1$. Let $\phi_i = \text{diag}(\mathbf{g}_r^H)\mathbf{g}_{u,i}$ and $\mathbf{v}_{d,i} = [v_{d,i,1}, \dots, v_{d,i,K}]^H$. Then, $|\mathbf{g}_r^H \Theta_{d,i} \mathbf{g}_{u,i} + g_{h,i}|^2$ can be rewritten as $|\mathbf{v}_{d,i}^H \phi_i + g_{h,i}|^2 = \mathbf{v}_{d,i}^H \phi_i \phi_i^H \mathbf{v}_{d,i} + \mathbf{v}_{d,i}^H \phi_i g_{h,i} + g_{h,i} \phi_i^H \mathbf{v}_{d,i} + |g_{h,i}|^2$. Thus, **P2** is reformulated as

$$\begin{aligned} \max_{\mathbf{v}_{d,i}} \quad & \mathbf{v}_{d,i}^H \phi_i \phi_i^H \mathbf{v}_{d,i} + \mathbf{v}_{d,i}^H \phi_i g_{h,i} + g_{h,i} \phi_i^H \mathbf{v}_{d,i} + |g_{h,i}|^2, \\ \text{s.t.} \quad & |v_{d,i,k}| = 1, \quad \forall k. \end{aligned} \tag{P2.1}$$

Note that **P2.1** is non-convex and difficult to be solved directly. Hence, we introduce an auxiliary matrix $\mathbf{R}_{d,i}$ and an auxiliary vector $\bar{\mathbf{v}}_{d,i}$ for mathematical manipulation, which are given by

$$\mathbf{R}_{d,i} = \begin{bmatrix} \phi_i \phi_i^H & \phi_i g_{h,i}^H \\ \phi_i^H g_{h,i} & 0 \end{bmatrix}, \quad \bar{\mathbf{v}}_{d,i} = \begin{bmatrix} \mathbf{v}_{d,i} \\ 1 \end{bmatrix}.$$

Based on $\mathbf{R}_{d,i}$ and $\bar{\mathbf{v}}_{d,i}$, the objective function of **P2.1** is rewritten as $\bar{\mathbf{v}}_{d,i}^H \mathbf{R}_{d,i} \bar{\mathbf{v}}_{d,i} + |g_{h,i}|^2 = \text{Tr}(\mathbf{R}_{d,i} \bar{\mathbf{v}}_{d,i} \bar{\mathbf{v}}_{d,i}^H) + |g_{h,i}|^2$. **P2.1** can be then expressed as

$$\begin{aligned} \max_{\bar{\mathbf{v}}_{d,i}} \quad & \text{Tr}(\mathbf{R}_{d,i} \bar{\mathbf{v}}_{d,i} \bar{\mathbf{v}}_{d,i}^H) + |g_{h,i}|^2, \\ \text{s.t.} \quad & |v_{d,i,k}| = 1, \quad \forall k. \end{aligned} \tag{P2.2}$$

Let $\mathbf{V}_{d,i} = \bar{\mathbf{v}}_{d,i} \bar{\mathbf{v}}_{d,i}^H$, where $\mathbf{V}_{d,i} \succeq 0$ and $\text{rank}(\mathbf{V}_{d,i}) = 1$. **P2.2** is then equivalent to

$$\begin{aligned} \max_{\mathbf{V}_{d,i}} \quad & \text{Tr}(\mathbf{R}_{d,i} \mathbf{V}_{d,i}) + |g_{h,i}|^2, \\ \text{s.t.} \quad & \text{C10: } \mathbf{V}_{d,i,k,k} = 1, \quad \forall k, \\ & \text{C11: } \mathbf{V}_{d,i} \succeq 0, \\ & \text{C12: } \text{rank}(\mathbf{V}_{d,i}) = 1, \end{aligned} \tag{P2.3}$$

where $\mathbf{V}_{d,i,k,k}$ denotes the k -th diagonal element of $\mathbf{V}_{d,i}$. **P2.3** is still a non-convex due to the rank-one constraint in C12. However, using the semidefinite relaxation (SDR) technique [28], we can relax the rank-one constraint to obtain a convex semidefinite programming (SDP) problem [29], which can be optimally solved using convex optimization toolboxes, e.g., CVX [30]. However, the solution obtained for the relaxed version of **P2.3** by CVX may not satisfy the rank-one constraint. To achieve a rank-one solution, i.e., an approximate solution with satisfying accuracy for **P2.3** (**P2.2**), the Gaussian randomization method is employed, which can construct a rank-one solution from the solution obtained by CVX.

Denote the solution to the relaxed problem as $\bar{\mathbf{V}}_{d,i}$. The singular value decomposition (SVD) of $\bar{\mathbf{V}}_{d,i}$ is expressed as $\bar{\mathbf{V}}_{d,i} = \mathbf{U}_{d,i} \mathbf{\Sigma}_{d,i} \mathbf{U}_{d,i}^H$, where $\mathbf{U}_{d,i} \in \mathcal{C}^{(K+1) \times (K+1)}$ and $\mathbf{\Sigma}_{d,i} \in \mathcal{C}^{(K+1) \times (K+1)}$ are the unitary matrix and diagonal matrix, respectively. Then, the approximate solution for **P2.2**, denoted by $\hat{\mathbf{v}}_i$, can be constructed as follows

$$\hat{\mathbf{v}}_{d,i} = \mathbf{U}_{d,i} \sqrt{\mathbf{\Sigma}_{d,i}} \mathbf{r}_{d,i}, \quad (17)$$

where $\mathbf{r}_{d,i}$ is a random vector with $\mathbf{r}_{d,i} \sim \mathcal{CN}(\mathbf{0}, \mathbf{I}_{K+1})$. We generate D_1 times of random vectors and compute the corresponding objective values for **P2.2**. The near-optimal solution to **P2.2**, $\hat{\mathbf{v}}_{d,i}^*$, is the one achieving the maximum objective function value of **P2.2**. The near-optimal solution to **P2.1**, denoted by $\mathbf{v}_{d,i}^*$, is finally recovered by

$$\mathbf{v}_{d,i}^* = e^{j \arg \left(\left[\begin{array}{c} \hat{\mathbf{v}}_{d,i}^* \\ \hat{\mathbf{v}}_{d,i,K+1}^* \end{array} \right]_{(1:K)} \right)}, \quad (18)$$

where $[\boldsymbol{\omega}]_{(1:M)}$ represents that the first M elements of $\boldsymbol{\omega}$ are taken, $\hat{\mathbf{v}}_{d,i,K+1}^*$ denotes the $(K+1)$ -th element of $\hat{\mathbf{v}}_{d,i}^*$ [20]. According to [31], the SDR technique followed by quite large number of randomizations based on the Gaussian randomization method can guarantee at least an $\frac{\pi}{4}$ approximation of the maximum objective function value of **P2.1**.

Algorithm 1 outlines the procedure for optimizing the IRS phase shift design in the IT phase.

Algorithm 1 The Algorithm for Solving **P2**.

- 1: Initialize D_1 , which is a large number of generating random vectors.
 - 2: Use the SDR technique and solve the relaxed version of **P2.3** by CVX to obtain $\bar{\mathbf{V}}_{d,i}$.
 - 3: Compute the SVD of $\bar{\mathbf{V}}_{d,i}$ and obtain $\mathbf{U}_{d,i}$ and $\mathbf{\Sigma}_{d,i}$.
 - 4: Initialize $\mathcal{Q} = \emptyset$.
 - 5: **for** $\bar{D} = 1 : D_1$ **do**
 - 6: Generate $\hat{\mathbf{v}}_{d,i}$ by (17).
 - 7: Compute the objective function of **P2.2** based on $\hat{\mathbf{v}}_{d,i}$ and denote it by $Q(\bar{D})$.
 - 8: $\mathcal{Q} = \mathcal{Q} \cup Q(\bar{D})$.
 - 9: **end for**
 - 10: Return $\hat{\mathbf{v}}_{d,i}^* = \arg \max_{\hat{\mathbf{v}}_{d,i}} \mathcal{Q}$.
 - 11: Compute $\mathbf{v}_{d,i}^*$ based on (18) given $\hat{\mathbf{v}}_{d,i}^*$, and extract $\boldsymbol{\theta}_{d,i}^*$.
-

According to Lemma 1, we can further obtain the following corollary.

Corollary 1. *The optimal phase shifts for the IT will align the signal of the HAP-IRS- U_i link with the*

signal of the HAP- U_i link, i.e.,

$$\mathbf{g}_r^H \Theta_{d,i} \mathbf{g}_{u,i} = \delta g_{h,i}, \quad (19)$$

where δ is a positive scalar.²

Proof. Refer to Appendix B. □

Remark 1. From Corollary 1, we can observe that for a given $P_{u,i}$, the received SNR at the HAP during t_i with the assistance of the IRS can be enhanced up to $(1 + \delta)^2$ compared with that of without IRS. It should be noted that δ is usually proportional to the number of reflecting elements. Hence, the system sum-rate can be significantly improved with the assistance of the IRS consisting of a large number of reflecting elements.

2) *Optimizing phase shift design for ET, time scheduling, and power allocation* : According to Lemma 1, **P1** can be simplified as

$$\begin{aligned} \max_{\mathbf{t}, \tau, \theta_e, P_u} \quad & \sum_{i=1}^N t_i \log_2 \left(1 + \frac{P_{u,i} \bar{\gamma}_i}{\sigma_h^2} \right), \\ \text{s.t.} \quad & \text{C1} - \text{C8}, \end{aligned} \quad (\mathbf{P3})$$

where $\bar{\gamma}_i = |\mathbf{g}_r^H \Theta_{d,i}^* \mathbf{g}_{u,i} + g_{h,i}|^2$, and $\Theta_{d,i}^*$ is obtained via Algorithm 1. **P3** is still non-convex because the variables are coupled in the objective function and the constraints. We introduce auxiliary variables $v_{e,k} = e^{j\theta_{e,k}}$, $\forall k$ and $e_{u,i} = P_{u,i} t_i$, $\forall i$. We also set $\psi_i = \text{diag}(\mathbf{h}_{u,i}^H) \mathbf{h}_r$. Then, we have $\mathbf{v}_e = [v_{e,1}, \dots, v_{e,K}]^H$, and $\mathbf{e}_u = [e_{u,1}, \dots, e_{u,N}]$. Let $\bar{\mathbf{v}}_e = [\mathbf{v}_e^H, 1]^H$ and $\mathbf{V}_e = \bar{\mathbf{v}}_e \bar{\mathbf{v}}_e^H$, where $\mathbf{V}_e \succeq 0$ and $\text{rank}(\mathbf{V}_e) = 1$. Based on these new variables, the constraint C2 is recast as follows:

$$\begin{aligned} \text{C13: } e_{u,i} + P_{c,i} t_i &\leq \eta P_h |h_{h,i}|^2 \tau_0 \\ &+ \eta P_h [\text{Tr}(R_{e,i} \mathbf{V}_e) + |h_{h,i}|^2] \tau_1, \quad \forall i, \end{aligned} \quad (20)$$

where

$$\mathbf{R}_{e,i} = \begin{bmatrix} \psi_i \psi_i^H & \psi_i h_{h,i}^H \\ \psi_i^H h_{h,i} & 0 \end{bmatrix}.$$

²From Corollary 1, we find that solving **P2** is equivalent to finding the optimal value of δ defined in (19).

Then, **P3** can be rewritten as

$$\begin{aligned}
& \max_{t, \tau, \mathbf{V}_e, \mathbf{e}_u} \sum_{i=1}^N t_i \log_2 \left(1 + \frac{e_{u,i} \bar{\gamma}_i}{t_i \sigma_h^2} \right), \\
& \text{s.t. C1, C3 – C6, C13,} \\
& \text{C14: } e_{u,i} \geq 0, \forall i, \\
& \text{C15: } \mathbf{V}_e \succeq 0, \\
& \text{C16: } \text{rank}(\mathbf{V}_{e,i}) = 1, \forall i.
\end{aligned} \tag{P3.1}$$

Due to the rank-one constraint in C16 and coupling of \mathbf{V}_e and τ_1 in C13, **P3.1** is still non-convex and difficult to be solved directly. However, it is straightforward to obtain the optimal duration of the first sub-slot in the ET phase, i.e., τ_0 , as stated in the following proposition.

Proposition 1. *The optimal duration of the first sub-slot in the ET phase can be obtained as*

$$\tau_0^* = \frac{K\mu}{K\mu + \eta P_h \|\mathbf{h}_r\|^2}. \tag{21}$$

Proof. Refer to Appendix C. □

Remark 2. *From Proposition 1, we can observe that the duration of the first sub-slot in the ET phase is mainly determined by the IRS's setting, e.g., the number of passive reflecting elements, each element's circuit power consumption, and the channel power gain between the HAP and IRS. If each element has a higher circuit power consumption, the IRS needs more time to harvest sufficient energy, which leaves shorter time for other network operations, i.e., users' EH with the assistance of IRS and users' IT. However, adding the number of elements may not increase the IRS's EH time because each element can harvest energy from the HAP individually.*

We now proceed to solve **P3.1** with τ_0^* obtained in Proposition 1. For solving **P3.1**, we first fix τ_1 and optimize time and energy allocation in the IT phase as well as the IRS phase shift design for the ET phase. We can then find the optimal τ_1 by a one-dimensional search over $[0, 1 - \tau_0] = [0, 1 - K\mu / (K\mu + \eta P_h \|\mathbf{h}_r\|^2)]$.

With fixed τ_1 , **P3.1** is reformulated as

$$\begin{aligned} \max_{\bar{\mathbf{t}}, \mathbf{V}_e, \mathbf{e}_u} \quad & \sum_{i=1}^N t_i \log_2 \left(1 + \frac{e_{u,i} \bar{\gamma}_i}{t_i \sigma_h^2} \right), \\ \text{s.t.} \quad & \text{C1, C6, C13} - \text{C16}, \\ & \sum_{i=1}^N t_i \leq 1 - \tau_0^* - \tau_1. \end{aligned} \tag{P3.2}$$

where $\bar{\mathbf{t}} = [t_1, \dots, t_N]$.

Relaxing the rank-one constraint in C16, **P3.2** will be a convex optimization problem [29]. We thus use the CVX tool [30] to solve the relaxed **P3.2** and obtain its optimal solution $\{t_1^*, \dots, t_N^*, \bar{e}_{u,1}, \dots, \bar{e}_{u,N}, \bar{\mathbf{V}}_e\}$. Similar to **P2.3**, the obtained $\bar{\mathbf{V}}_e$ generally does not satisfy the rank-one constraint. Hence, the Gaussian randomization method is adopted to construct an approximate rank-one solution, which is given by

$$\hat{\mathbf{v}}_e = \mathbf{U}_e \sqrt{\Sigma_e} \mathbf{r}_e, \tag{22}$$

where $\mathbf{U}_e \in \mathcal{C}^{(K+1) \times (K+1)}$ and $\Sigma_e \in \mathcal{C}^{(K+1) \times (K+1)}$ are the unitary matrix and diagonal matrix resulting from SVD of $\bar{\mathbf{V}}_e$, and $\mathbf{r}_e \sim \mathcal{CN}(\mathbf{0}, \mathbf{I}_{K+1})$. Note that as the objective function is an increasing function of $e_{u,i}$, C13 must be active at the optimal solution. Therefore, based on the generated random vectors, the energy allocation of the users is computed as

$$\begin{aligned} \hat{e}_{u,i} = & \left(\eta P_h |h_{h,i}|^2 \tau_0^* + \eta P_h \text{Tr}(\mathbf{R}_{e,i} \hat{\mathbf{v}}_e \hat{\mathbf{v}}_e^H) \tau_1 \right. \\ & \left. + \eta P_h |h_{h,i}|^2 \tau_1 - P_{c,i} t_i^* \right)^+, \quad \forall i, \end{aligned} \tag{23}$$

where $(x)^+$ means $\max(x, 0)$. Finally, $\hat{\mathbf{v}}_e^*$ is the vector achieving the maximum objective function value and $e_{u,i}^*, \forall i$ is the corresponding energy allocation solution obtained from (23).

The procedure for solving the sum-rate maximization problem for the TS scheme is summarized in Algorithm 2. By running Algorithm 2, we can obtain the near-optimal solution for **P1**. Note that the accuracy of our obtained solution is related with the number of randomizations for the Gaussian randomization method used in each sub-problem and the step-size for updating t_1 in the second sub-problem. Hence, we can achieve a solution for **P1** with satisfying accuracy by increasing the number of randomizations and using a smaller step-size.

Algorithm 2 The Algorithm for Solving **P1**.

- 1: Initialize D_2 and the step size Δ . Let $\tau_1 = 0$.
 - 2: Find the optimal phase shifts for the IT phase from Algorithm 1 and optimal τ_0 from Proposition 1.
 - 3: **while** $\tau_1 \leq 1 - K\mu/(K\mu + \eta P_h \|\mathbf{h}_r\|^2)$ **do**
 - 4: Solve the relaxed version of **P3.2** with fixed τ_1 and obtain its optimal solution $\bar{\mathbf{V}}_e$.
 - 5: Compute the SVD of $\bar{\mathbf{V}}_e$ and obtain \mathbf{U}_e and $\mathbf{\Sigma}_e$.
 - 6: **for** $\bar{D} = 1 : D_2$ **do**
 - 7: Generate $\hat{\mathbf{v}}_e$ by (22) and find $\hat{e}_{u,i}$, $\forall i$ from (23).
 - 8: Calculate the objective function value of **P3.2** and denote it by $R_{\text{sum}}(\bar{D})$.
 - 9: **end for**
 - 10: Set $R^*(\tau_1) = \max R_{\text{sum}}$.
 - 11: $\tau_1 = \tau_1 + \Delta$.
 - 12: **end while**
 - 13: Set $\tau_1^* = \arg \max_{\tau_1} R^*$, $\mathbf{v}_e^* = \mathbf{v}_e^*(\tau_1^*)$, $\mathbf{e}_u^* = \mathbf{e}_u^*(\tau_1^*)$, $\bar{\mathbf{t}}^* = \bar{\mathbf{t}}^*(\tau_1^*)$.
 - 14: Set $P_{u,i}^* = e_{u,i}^*/t_i^*$, $\forall i$ and extract $\theta_{e,k}^*$, $\forall k$ from \mathbf{v}_e^* .
 - 15: Return τ_0^* , τ_1^* , $\bar{\mathbf{t}}^*$, \mathbf{P}_u^* , $\boldsymbol{\theta}_e^*$ and $\boldsymbol{\theta}_{d,i}^*$, $\forall i$.
-

B. Random phase shifts with optimized resource allocation for the TS scheme

To reduce the computational complexity and show more insights about resource allocation, we consider a special case with random design of phase shifts and focus on the time and power allocation optimization in the IRS-assisted WPCN. As will be shown in Section V, using IRS is beneficial for improving the performance of WPCN even with randomly designed phase shifts [15], [32]. Letting $e_{u,i} = P_{u,i}t_i$ and $\gamma_{u,i} = |\mathbf{h}_{u,i}^H \bar{\boldsymbol{\Theta}}_e \mathbf{h}_r + h_{h,i}|^2$, we have

$$\text{C17: } e_{u,i} + P_{c,i}t_i \leq \eta P_h |h_{h,i}|^2 \tau_0 + \eta P_h \gamma_{u,i} \tau_1, \quad \forall i, \quad (24)$$

and the sum-rate maximization problem with random phase shifts is formulated as

$$\begin{aligned} \max_{\mathbf{t}, \tau, \mathbf{e}_u} \quad & \sum_{i=1}^N t_i \log_2 \left(1 + \frac{\gamma_{d,i} e_{u,i}}{\sigma_h^2 t_i} \right), \\ \text{s.t.} \quad & \text{C1, C3 - C6, C17, } e_{u,i} \geq 0, \forall i, \end{aligned} \quad (\text{P4})$$

where $\gamma_{d,i} = |\mathbf{g}_r^H \boldsymbol{\Theta}_{d,i} \mathbf{g}_{u,i} + g_{h,i}|^2$. The constraint C17 is an equality at the optimal solution as we discussed earlier. Hence, we have

$$e_{u,i}^* = \eta P_h |h_{h,i}|^2 \tau_0^* + \eta P_h \gamma_{u,i} \tau_1^* - P_{c,i} t_i^*, \quad \forall i \quad (25)$$

Substituting (25) into R_i , we have

$$R_i = t_i \log_2 \left(1 + \frac{a_i + b_i \tau_1}{t_i} - c_i \right), \quad (26)$$

where $a_i = \eta P_h |h_{h,i}|^2 \gamma_{d,i} \tau_0 / \sigma_h^2$, $b_i = \eta P_h \gamma_{u,i} \gamma_{d,i} / \sigma_h^2$ and $c_i = P_{c,i} \gamma_{d,i} / \sigma_h^2$. Proposition 1 holds here as well.

Hence, **P4** is modified as

$$\begin{aligned} \max_{\bar{\mathbf{t}}, \tau_1} \quad & \sum_{i=1}^N t_i \log_2 \left(1 + \frac{a_i + b_i \tau_1}{t_i} - c_i \right), \\ \text{s.t.} \quad & \text{C4, C6, } \tau_1 \geq 0, \end{aligned} \quad (\mathbf{P4.1})$$

It can be verified that **P4.1** is a convex optimization problem [29], which can be solved by standard convex optimization techniques, e.g., Lagrange duality method. The Lagrangian of **P4.1** is given by

$$\begin{aligned} \mathcal{L}(\bar{\mathbf{t}}, \rho, \tau_1) = & \sum_{i=1}^N t_i \log_2 \left(1 + \frac{a_i + b_i \tau_1}{t_i} - c_i \right) \\ & - \rho \left[\tau_0 + \tau_1 + \sum_{i=1}^N t_i - 1 \right], \end{aligned} \quad (27)$$

where $\rho \geq 0$ is the Lagrange multiplier associated with the constraint C4.

Proposition 2. *With random design of phase shifts, the optimal time scheduling for the TS scheme is given by*

$$\tau_1^* = \frac{1 - \frac{K\mu}{K\mu + \eta P_h \|\mathbf{h}_r\|^2} - \sum_{i=1}^N \frac{a_i}{z_i^* + c_i}}{1 + \sum_{i=1}^N \frac{b_i}{z_i^* + c_i}}, \quad (28)$$

$$t_i^* = \frac{a_i + b_i \tau_1^*}{z_i^* + c_i}, \quad \forall i, \quad (29)$$

where $z_i^* > 0$ is the unique solution of

$$\log_2(1 + z_i) - \frac{z_i + c_i}{\ln(2)(1 + z_i)} = \rho^*, \quad (30)$$

and ρ^* is the optimal dual variable.

Proof. Refer to Appendix D. □

Using (25) and Propositions 1 and 2, the optimal energy allocation at each user can be easily obtained.

IV. SUM-RATE MAXIMIZATION FOR THE PS SCHEME

In this section, we investigate the optimal solution to the sum-rate maximization problem for the PS scheme. The problem is formulated as

$$\begin{aligned}
& \max_{\mathbf{t}, \boldsymbol{\theta}_e, \{\boldsymbol{\theta}_{d,i}\}_{i=1}^N, \mathbf{P}_u, \beta_e} \sum_{i=1}^N R_i, \\
& \text{s.t. C4, C6 – C9,} \\
& \text{C18: } K\mu(t_0 + \sum_{i=1}^N t_i) \leq E_{ps,r}, \quad \forall i, \\
& \text{C19: } P_{u,i}t_i + P_{c,i}t_i \leq E_{ps,i}, \quad \forall i, \\
& \text{C20: } 0 \leq \beta_e \leq 1.
\end{aligned} \tag{P5}$$

A. Optimal solution to P5

Similar to **P1**, **P5** is a non-convex optimization problem due to the coupled variables in the objective function and the constraints. It is straightforward to observe that Lemma 1 also holds for **P5**. Hence, the optimal phase shifts for the IT phase can be found from Algorithm 1. Accordingly, **P5** can be reformulated as

$$\begin{aligned}
& \max_{\mathbf{t}, \boldsymbol{\theta}_e, \mathbf{P}_u, \beta_e} \sum_{i=1}^N t_i \log_2 \left(1 + \frac{P_{u,i} \tilde{\gamma}_i}{\sigma_h^2} \right), \\
& \text{s.t. C4, C6 – C8, C18 – C20.}
\end{aligned} \tag{P5.1}$$

Lemma 2. *To guarantee that the value of sum-rate for the PS scheme is greater than zero, the following condition that the maximum harvested energy at the IRS from the HAP is larger than its circuit power consumption must be satisfied, i.e.,*

$$K\mu < \eta P_h \|\mathbf{h}_r\|^2. \tag{31}$$

Proof. Refer to Appendix E. □

Remark 3. *From Lemma 2, we can observe that unlike the TS scheme, the PS scheme cannot always be used, i.e., if (31) is not satisfied. However, we can increase the transmit power at the HAP and/or reduce the distance between the HAP and IRS to enable the PS scheme.*

In the following, we investigate **P5.1** under the condition that (31) is satisfied, because otherwise, using IRS would be infeasible. Following the same steps as in Section III-A2, the sum-rate maximization

problem is formulated as

$$\begin{aligned}
& \max_{\mathbf{t}, e_u, \beta_e, \mathbf{V}_e} \sum_{i=1}^N t_i \log_2 \left(1 + \frac{\bar{\gamma}_i}{\sigma_h^2} \frac{e_{u,i}}{t_i} \right), \\
& \text{s.t. C4, C6, C14, C18, C20,} \\
& \text{C21: } e_{u,i} + P_{c,i} t_i \leq \eta P_h [\text{Tr}(\bar{\mathbf{R}}_{e,i} \mathbf{V}_e) + |h_{h,i}|^2] t_0, \\
& \mathbf{V}_e \succeq 0, \\
& \text{rank}(\mathbf{V}_e) = 1.
\end{aligned} \tag{P5.2}$$

where

$$\bar{\mathbf{R}}_{e,i} = \begin{bmatrix} \beta_e^2 \boldsymbol{\psi}_i \boldsymbol{\psi}_i^H & \beta_e \boldsymbol{\psi}_i h_{h,i}^H \\ \beta_e \boldsymbol{\psi}_i^H h_{h,i} & 0 \end{bmatrix}.$$

Proposition 3. *The optimal value of the amplitude reflection coefficient β_e is obtained as*

$$\beta_e^* = \sqrt{1 - \frac{K\mu}{\eta P_h \|\mathbf{h}_r\|^2 t_0^*}}, \tag{32}$$

where $\frac{K\mu}{\eta P_h \|\mathbf{h}_r\|^2} < t_0^* \leq 1$.

The proof of Proposition 3 is similar to that of Proposition 1 and is thus omitted for brevity.

Remark 4. *According to Proposition 3, t_0 is increasing with respect to β . It is because a larger β makes the instantaneous harvested power by the IRS be reduced so that the IRS needs more time to harvest sufficient energy. For the scenario that the transmit power at the HAP is small, a longer duration for the ET phase is required.*

For solving **P5.2**, we first fix t_0 and optimize other variables. The optimal value of t_0 can then be obtained by a one-dimensional search over $(K\mu/(\eta P_h \|\mathbf{h}_r\|^2), 1]$.

Given t_0 , the optimal value of β_e can be found from Proposition 3 and we will have the following optimization problem:

$$\begin{aligned}
& \max_{\mathbf{t}, e_u, \mathbf{V}_e} \sum_{i=1}^N t_i \log_2 \left(1 + \frac{\bar{\gamma}_i}{\sigma_h^2} \frac{e_{u,i}}{t_i} \right), \\
& \text{s.t. C4, C14, C21,} \\
& \mathbf{V}_e \succeq 0, \\
& \text{rank}(\mathbf{V}_e) = 1.
\end{aligned} \tag{P5.3}$$

After the relaxation of the rank-one constraint, problem **P5.3** is similar to **P3.2** in Section III-A2 and can be solved following the same procedure. For brevity and to avoid repetition, we do not explain the details of solving problem **P5.3** here.

Algorithm 3 describes the process of solving the sum-rate maximization problem for the PS scheme (**P5**).

Algorithm 3 The Algorithm for Solving **P5**.

- 1: Initialize $t_0 = K\mu/(\eta P_h \|\mathbf{h}_r\|^2)$, Δ and $R^* = 0$.
 - 2: Find the optimal phase shifts for the IT phase from Algorithm 1.
 - 3: **repeat**
 - 4: Obtain $\beta_e^*(t_0)$ from (32).
 - 5: Solve **P5.3** to obtain $\bar{\mathbf{t}}^*(t_0)$, $\mathbf{e}_u^*(t_0)$, and $\mathbf{V}_e^*(t_0)$.
 - 6: calculate $R^*(t_0) = \sum_{i=1}^N R_i^*(t_0)$.
 - 7: $t_0 = t_0 + \Delta$.
 - 8: **until** $t_0 > 1$.
 - 9: Set $t_0^* = \arg \max_{t_0} R^*$, $\beta_e^* = \beta_e^*(t_0^*)$, $\bar{\mathbf{t}}^* = \bar{\mathbf{t}}^*(t_0^*)$, $\mathbf{e}_u^* = \mathbf{e}_u^*(t_0^*)$, $\mathbf{V}_e^* = \mathbf{V}_e^*(t_0^*)$.
 - 10: Set $P_{u,i}^* = e_{u,i}^*/t_i^*$, $\forall i$ and extract $\theta_{e,k}^*$, $\forall k$ from \mathbf{V}_e^* .
 - 11: Return t_0^* , β_e^* , $\bar{\mathbf{t}}^*$, \mathbf{P}_u^* , θ_e^* , and $\theta_{d,i}^*$.
-

B. Random phase shifts with optimized resource allocation for the PS scheme

Similar to Section III-B, we consider the random design of phase shifts for the PS scheme and optimize the resource allocation in the network. With randomly generated phase shifts and after setting $e_{u,i} = P_{u,i}t_i$, $\forall i$, we have the following resource allocation problem:

$$\begin{aligned} \max_{\mathbf{t}, \mathbf{e}_u, \beta_e} \quad & \sum_{i=1}^N t_i \log_2 \left(1 + \frac{\gamma_{d,i} e_{u,i}}{\sigma_h^2 t_i} \right), \\ \text{s.t.} \quad & \text{C4, C6, C14, C18, C20,} \\ & \text{C22: } e_{u,i} + P_{c,i}t_i \leq \eta P_h \bar{\gamma}_{u,i} t_0, \quad \forall i, \end{aligned} \tag{P6}$$

where $\bar{\gamma}_{u,i} = |\mathbf{h}_{u,i}^H \beta_e \bar{\Theta}_e \mathbf{h}_r + h_{h,i}|^2$. It can be observed that Proposition 3 also holds for **P6**. Due to the non-convexity of the constraint C22, it is still challenging to solve **P6**. Hence, we also first fix t_0 and optimize the time and energy allocation in the IT phase. We then find the optimal value of t_0 by searching over $(K\mu/(\eta P_h \|\mathbf{h}_r\|^2), 1]$.

We know from previous discussions that C22 must be met with equality at the optimal solution, i.e.,

$$e_{u,i}^* + P_{c,i}t_i^* = \eta P_h \bar{\gamma}_{u,i} t_0^*. \tag{33}$$

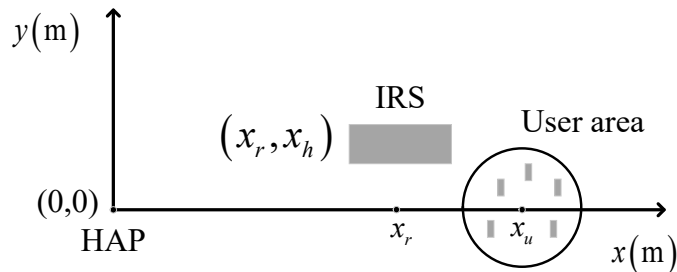


Fig. 3. Simulation setup for the IRS-assisted WPCN.

Consequently, given t_0 and β_e , **P6** is rewritten as

$$\begin{aligned} \max_{\bar{\mathbf{t}}} \quad & \sum_{i=1}^N t_i \log_2(1 + d_i \frac{t_0}{t_i} - c_i), \\ \text{s.t.} \quad & \text{C4, C6,} \end{aligned} \tag{P6.1}$$

where $d_i = \eta P_h \gamma_{d,i} \bar{\gamma}_{u,i} / \sigma_h^2$. The Lagrangian of the above convex problem is given by

$$\mathcal{L}(\bar{\mathbf{t}}, \zeta) = \sum_{i=1}^N t_i \log_2(1 + d_i \frac{t_0}{t_i} - c_i) - \zeta (t_0 + \sum_{i=1}^N t_i - 1), \tag{34}$$

where ζ is the Lagrange multiplier associated with the constraint C4.

Proposition 4. *With fixed t_0 and β_e , the optimal time allocation in the IT phase for the PS scheme is given by*

$$t_i^* = \frac{d_i}{w_i^* + c_i}, \quad \forall i, \tag{35}$$

where $w_i^* > 0$ is the unique solution of

$$\log_2(1 + w_i) - \frac{w_i + c_i}{\ln(2)(1 + w_i)} = \zeta^*, \tag{36}$$

and ζ^* is the optimal dual variable.

The proof of Proposition 4 is similar to that of Proposition 2 and is thus omitted for brevity. The optimal energy allocation can then be easily found via (33) and Proposition 4.

V. PERFORMANCE EVALUATION

In this section, we present numerical results to evaluate the performance of the proposed solutions for the IRS-assisted WPCN. The simulated network topology is a 2-D coordinate system as shown in Fig.

3, where the coordinates of the HAP and the IRS are given as $(0,0)$ and (x_r, x_h) , the users are randomly deployed within a circular area centered at $(x_u, 0)$ with radius 2 m. The large-scale path-loss is modeled as $A(d/d_0)^{-\alpha}$, where A is the path-loss at the reference distance $d_0 = 1$ m and set to $A = -10$ dB, d denotes the distance between two nodes, and α is the path-loss exponent. The path-loss exponents of the links between the HAP and users are assumed to be 3.6 since the users are randomly deployed, while the path-loss exponents of the links between the HAP and IRS and between the IRS and users are set as 2.2 because the IRS can be carefully deployed to avoid the severe signal blockage [17]. The small-scale channel coefficients are generated as circularly symmetric Gaussian random variables with zero mean and unit variance. The results are obtained by averaging over different channel realizations.

Unless otherwise stated, other parameters are given as follows: $\eta = 0.8$, $\sigma_h^2 = -110$ dBm, $\mu = 1$ dBm, $P_{c,i} = 5$ dBm, $N = 3$, $K = 20$, $P = 30$ dBm, $x_r = 3$ m, $x_h = 0.5$ m, and $x_u = 10$ m. The scheme with random design of phase shifts and the scheme without IRS are used as benchmarks for performance comparisons.

Fig. 4 shows the influence of HAP's transmit power on the average system sum-rate. As expected, the sum-rate is improved with the increase of the HAP's transmit power because the users can harvest more energy when the HAP's transmit power is higher. Further, according to Proposition 1, the time needed for the IRS's EH in the TS scheme is reduced when the transmit power of the HAP is increased. This gives more time for the IRS to assist in downlink ET from the HAP to the users, which boosts the harvested energy at the user and consequently improves the sum-rate. As for the PS scheme, increasing the HAP's transmit power results in higher amplitude reflection coefficient according to Proposition 3, which enhances the users' harvested energy. It can be seen that our proposed schemes with optimized phase shift design outperform the benchmark ones for both the TS and PS schemes. We can also observe that the performance gap between the proposed optimized design and the benchmark schemes increases when the HAP's transmit power gets larger. The figure also shows that when $P \leq 20$ dBm, there is no gain in using IRS for improving the performance of WPCN for the PS method, which is consistent with what has been noted in Lemma 2. It is also worth mentioning that even the schemes with random phase shifts can bring performance gains to the conventional WPCN. That is because the RF energy can still be transferred from the HAP to the users through the reflecting links [32]. It endorses the effectiveness of using IRS for performance enhancement even if the channel knowledge of the IRS's links for optimized phase shift design is unavailable.

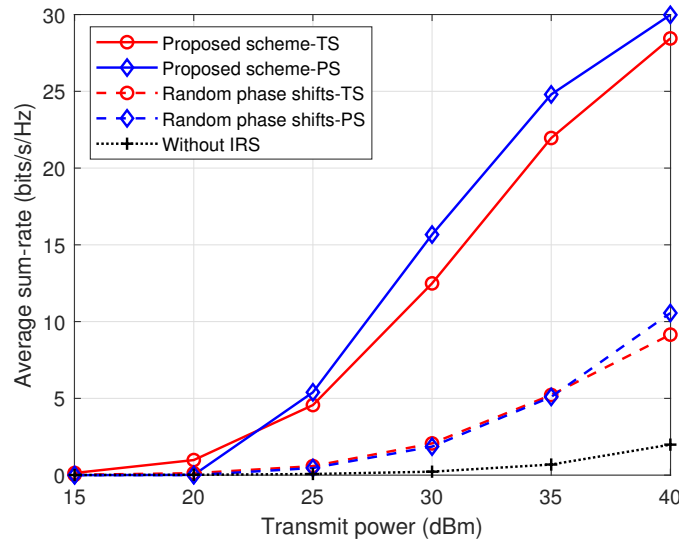


Fig. 4. Sum-rate versus HAP's transmit power.

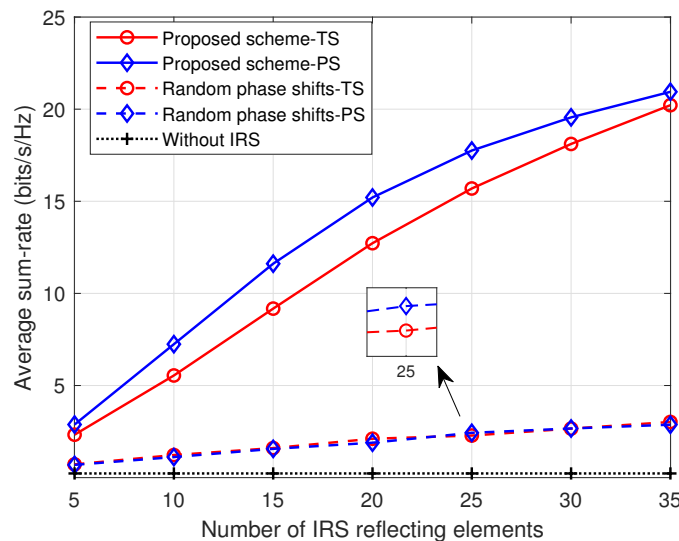


Fig. 5. Sum-rate versus number of IRS reflecting elements.

In Fig. 5, we study the impact of the number of IRS reflecting elements on the average sum-rate. It can be clearly observed that our proposed solutions can achieve a significant gain in terms of the average sum-rate compared with other schemes. For the scheme without IRS, the average sum-rate is very small. It is because the received power at each user from the HAP through the direct link only is much smaller than its circuit power consumption, thus most of the transmission block time is used to harvest energy to power its circuit, and the remaining energy and time for the IT is very limited. However, the received power from the HAP through the direct and reflecting links can be comparable to the circuit power consumption under our proposed scheme. Hence, each user has relatively sufficient energy and time to transmit data.

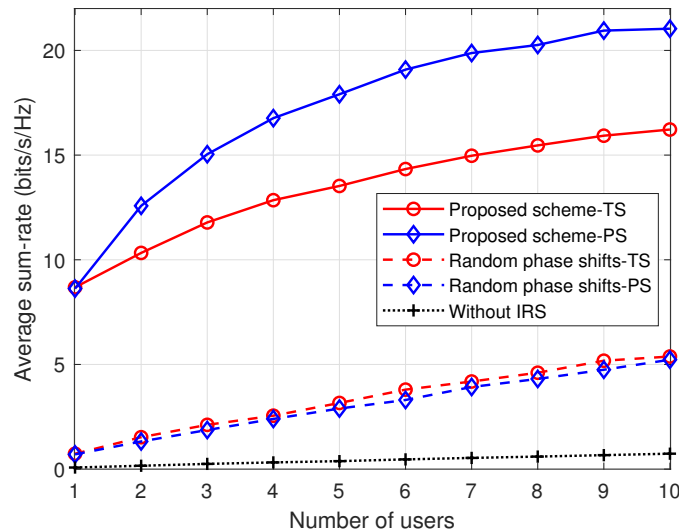


Fig. 6. Sum-rate versus number of users.

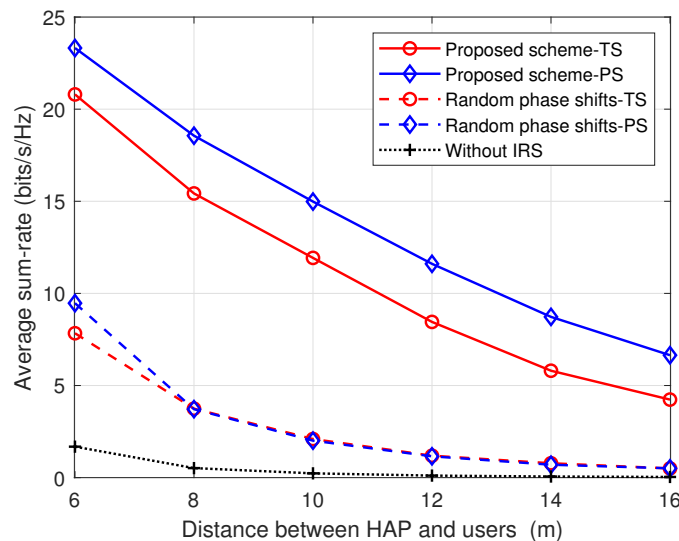


Fig. 7. Sum-rate versus distance between HAP and users.

With the increase of number of IRS elements, the received power at each user becomes larger, which leads to a better system performance.

Next, we study the effect of the number of network users on the average sum-rate in Fig. 6. Again, the proposed IRS-assisted WPCN with optimal phase shift design notably outperforms the other two schemes. It can be observed that the average sum-rate is increasing with the number of WPCN users because more energy can be harvested with the increase of the number of users. Nevertheless, the average sum-rate does not increase when the number of users reaches a high number, e.g., over 10 users. The reason for this observation is that adding new users implies that more time is needed for the IT phase, which in

consequence decreases the ET phase duration. Shorter ET duration in the TS scheme means that less time will be left for the IRS to assist in the downlink ET. In the PS scheme, the IRS needs to decrease its amplitude reflection coefficient β_e to compensate for the loss of energy incurred by shortening the ET duration. Therefore, the gain brought by incrementing the number of users is neutralized by shortened ET time and the average sum-rate converges to an upper bound.

Finally, we investigate the effect of users' location on the sum-rate performance. As shown in Fig. 7, increasing x_u results in sum-rate reduction because as x_u increases, the users move further from both the HAP and IRS. Therefore, the signals received by the users in the ET phase from both the HAP and the IRS become weaker. Similarly, the signals received by the HAP in the uplink IT also becomes weaker. Once again, the proposed schemes can significantly outperform the other two schemes.

VI. CONCLUSIONS

This paper has proposed the hybrid-relaying scheme empowered by a self-sustainable IRS to enhance the performance of WPCN, where the IRS is deployed to improve the efficiency of downlink ET from the HAP to a number of users and uplink IT from the users to the HAP. In addition, we have proposed the TS and PS schemes for the IRS to harvest sufficient energy from the HAP to power its operations and investigated system sum-rate maximization problems for both schemes. To address the non-convexity of each formulated problem, we have developed the two-step method to efficiently obtain the near-optimal solution with satisfying accuracy. The special problems with random phase shifts have also been investigated to reveal the structure of time and energy allocation. Then, we have performed simulations to evaluate the superiority of our proposed schemes, which have shown that our proposed schemes can achieve remarkable sum-rate gain compared to the baseline WPCN without IRS. From simulation results, we have also observed that the PS scheme can achieve a better performance than the TS scheme if the transmit power at the HAP is large enough or the channel between the HAP and IRS is strong. However, compared to the PS scheme, the TS scheme can be more widely applied because it is free from the constraint defined in Lemma 2 for the PS scheme.

APPENDIX A

PROOF OF LEMMA 1

It is straightforward that R_i is an increasing function with respect to $|\mathbf{g}_r^H \Theta_{d,i} \mathbf{g}_{u,i} + g_{h,i}|^2$ for $i = 1, \dots, N$. Therefore, at the optimal solution of **P1**, $|\mathbf{g}_r^H \Theta_{d,i} \mathbf{g}_{u,i} + g_{h,i}|^2$ must be maximized $\forall i$. In addition,

$|\mathbf{g}_r^H \Theta_{d,i} \mathbf{g}_{u,i} + g_{h,i}|^2$ only depends on $\theta_{d,i}$ ($\Theta_{d,i}$), where $0 \leq \theta_{d,i,k} \leq 2\pi$, $\forall k$. As a result, for any given and feasible \mathbf{t} and \mathbf{P}_u , maximizing the objective function of **P1** is equivalent to solving **P2** independently for $i = 1, \dots, N$. This thus proves Lemma 1.

APPENDIX B

PROOF OF COROLLARY 1

$|\mathbf{g}_r^H \Theta_{d,i} \mathbf{g}_{u,i} + g_{h,i}|^2$ can be rewritten as $|\mathbf{g}_r^H \Theta_{d,i} \mathbf{g}_{u,i}|^2 + |g_{h,i}|^2 + 2|\mathbf{g}_r^H \Theta_{d,i} \mathbf{g}_{u,i}||g_{h,i}| \cos \alpha$, where

$$\alpha = \arctan \frac{\text{Im}(\mathbf{g}_r^H \Theta_{d,i} \mathbf{g}_{u,i})}{\text{Re}(\mathbf{g}_r^H \Theta_{d,i} \mathbf{g}_{u,i})} - \arctan \frac{\text{Im}(g_{h,i})}{\text{Re}(g_{h,i})}. \quad (37)$$

It is obvious that the maximum of $|\mathbf{g}_r^H \Theta_{d,i} \mathbf{g}_{u,i} + g_{h,i}|^2$ is achieved if $\alpha = 0$, i.e., when $\mathbf{g}_r^H \Theta_{d,i} \mathbf{g}_{u,i}$ and $g_{h,i}$ are aligned. This thus proves Corollary 1.

APPENDIX C

PROOF OF PROPOSITION 1

It can be verified that the objective function of **P3.1** is an increasing function with respect to t_i for $i = 1, \dots, N$. Hence, at the optimal solution, the constraint C1 must be satisfied with equality. We can also observe that the right hand side of C1 is increasing with respect to τ_0 . Thus, the constraint C3 must be met with equality at the optimal solution because otherwise we can always increase τ_0 as a result of which t_i can be increased. Similarly, the constraint C4 must also be an equality at the optimal solution as otherwise we can increase t_0 , which leads to the increase of τ_0 . Based on the three equalities from the constraints C1, C3 and C4, we can straightforwardly obtain the optimal value of τ_0 as given by (21).

APPENDIX D

PROOF OF PROPOSITION 2

The dual function of **P4.1** is given by

$$\mathcal{G}(\rho) = \max_{\bar{\mathbf{t}} \geq 0, \tau_1 \geq 0} \mathcal{L}(\bar{\mathbf{t}}, \tau_1, \rho), \quad (38)$$

Karush-Kuhn-Tucker (KKT) conditions are both necessary and sufficient for the optimality of **P4.1** [29], which are given by

$$\begin{aligned} \frac{\partial \mathcal{L}}{\partial t_i} &= \log_2 \left(1 + \frac{a_i + b_i \tau_1^*}{t_i^*} - c_i \right) - \frac{\frac{a_i + b_i \tau_1^*}{t_i^*}}{\ln(2) \left(1 + \frac{a_i + b_i \tau_1^*}{t_i^*} - c_i \right)} \\ &\quad - \rho^* = 0, \end{aligned} \quad (39)$$

$$\frac{\partial \mathcal{L}}{\partial \tau_1} = \sum_{i=1}^N \frac{b_i}{\ln(2) \left(1 + \frac{a_i + b_i \tau_1^*}{t_i^*} - c_i \right)} - \rho^* = 0, \quad (40)$$

$$\rho^* \left[\tau_0 + \tau_1^* + \sum_{i=1}^N t_i^* - 1 \right] = 0. \quad (41)$$

Setting $z_i = \frac{a_i + b_i \tau_1}{t_i} - c_i$ and substituting it into (39) and (40), we have

$$\log_2(1 + z_i) - \frac{z_i + c_i}{\ln(2)(1 + z_i)} = \rho^*, \quad (42)$$

$$\sum_{i=1}^N \frac{b_i}{\ln(2)(1 + z_i)} = \rho^*. \quad (43)$$

It is straightforward to verify that the left hand side of (42) is a strictly increasing function with respect to $z_i > 0$. Hence, there exists a unique solution, denoted by z_i^* , satisfying (42). From (43), we can observe that ρ^* is upper-bounded by $\frac{1}{\ln(2)} \sum_{i=1}^N b_i$ and can be thus found by the bisection method. Also, (43) indicates that $\rho^* > 0$. Having $\tau_0 + \tau_1^* + \sum_{i=1}^N t_i^* = 1$ from (41) and $z_i^* = \frac{a_i + b_i \tau_1^*}{t_i^*} - c_i$, (28) and (29) are obtained with some simple mathematical calculations. This thus proves Proposition 2.

APPENDIX E

PROOF OF LEMMA 2

From C18, we have

$$\beta_e \leq \sqrt{1 - \frac{K\mu(\sum_{i=0}^N t_i)}{\eta P_h \|\mathbf{h}_r\|^2 t_0}}. \quad (44)$$

According to (44), for the value of β_e to be strictly positive, we must have

$$K\mu < \frac{\eta P_h \|\mathbf{h}_r\|^2 t_0}{\sum_{i=0}^N t_i} \leq \eta P_h \|\mathbf{h}_r\|^2. \quad (45)$$

Lemma 2 is thus proved.

REFERENCES

- [1] Cisco edge-to-enterprise IoT analytics for electric utilities. Available Online: <https://www.cisco.com/c/en/us/solutions/collateral/data-center-virtualization/big-data/solution-overview-c22-740248.html>, Feb. 2018.
- [2] X. Lu, P. Wang, D. Niyato, D. I. Kim, and Z. Han, "Wireless networks with RF energy harvesting: A contemporary survey," *IEEE Commun. Surv. Tut.*, vol. 17, no. 2, pp. 757-789, Secondquarter 2015.
- [3] H. Ju and R. Zhang, "Throughput maximization in wireless powered communication networks," *IEEE Trans. Wireless Commun.*, vol. 13, no. 1, pp. 418-428, Jan. 2014.
- [4] P. Ramezani and A. Jamalipour, "Toward the evolution of wireless powered communication networks for the future Internet of Things," *IEEE Network*, vol. 31, no. 6, pp. 62-69, Nov./Dec. 2017.
- [5] H. Chen, Y. Li, J. L. Rebelatto, B. F. Uchoa-Filho, and B. Vucetic, "Harvest-then-cooperate: Wireless-powered cooperative communications," *IEEE Trans. Signal Process.*, vol. 63, no. 7, pp. 1700-1711, Apr., 2015.
- [6] H. Ju and R. Zhang, "Uer cooperation in wireless powered communication networks," in *Proc. IEEE GLOBECOM*, Austin, TX, USA, Dec. 2014, pp. 1430-1435.
- [7] Y. Zeng, H. Chen, and R. Zhang, "Bidirectional wireless information and power transfer with a helping relay," *IEEE Commun. Letters*, vol. 20, no. 5, pp. 862-865, May 2016.
- [8] C. Zhong, H. A. Suraweera, G. Zheng, I. Krikidis, and Z. Zhang, "Wireless information and power transfer with full duplex relaying," *IEEE Trans. Commun.*, vol. 62, no. 10, pp. 3447-3461, Oct. 2014.
- [9] B. Lyu, D. T. Hoang, and Z. Yang, "User Cooperation in wireless-powered backscatter communication networks," *IEEE Wireless Commun. Lett.*, vol. 8, no. 2, pp. 632-635, Apr. 2019.
- [10] S. H. Kim and D. I. Kim, "Hybrid backscatter communication for wireless-powered heterogeneous networks," *IEEE Trans. Wireless Commun.*, vol. 16, no. 10, pp. 6557-6570, Oct. 2017.
- [11] S. Gong, X. Huang, J. Xu, W. Liu, P. Wang, and D. Niyato, "Backscatter relay communications powered by wireless energy beamforming," *IEEE Trans. Commun.*, vol. 66, no. 7, pp. 3187-3200, July 2018.
- [12] V. Liu, A. Parks, V. Talla, S. Gollakota, D. Wetherall, and J. R. Smith, "Ambient backscatter: Wireless communication out of thin air," in *Proc. SIGCOMM*, pp. 39-50, Hong Kong, Aug. 2013.
- [13] Q. Wu and R. Zhang, "Towards smart and reconfigurable environment: Intelligent reflecting surface aided wireless network," *IEEE Commun. Mag.*, vol. 58, no. 1, pp. 106-112, Jan. 2020.
- [14] S. Gong, X. Lu, D. T. Hoang, D. Niyato, L. Shu, D. I. Kim, and Y. C. Liang, "Towards smart radio environment for wireless communications via intelligent reflecting surfaces: A comprehensive survey". Available Online: <https://arxiv.org/pdf/1912.07794.pdf>, Dec. 2019.
- [15] Q. Wu and R. Zhang, "Intelligent reflecting surface enhanced wireless network via joint active and passive beamforming," *IEEE Trans. Wireless Commun.*, vol. 18, no. 11, pp. 5394-5409, Nov. 2019.
- [16] D. Mishra and H. Johansson, "Channel estimation and low-complexity beamforming design for passive intelligent surface assisted MISO wireless energy transfer," in *Proc. IEEE ICASSP*, Brighton, UK, May 2019, pp. 4659-4663.
- [17] Q. Wu and R. Zhang, "Weighted sum power maximization for intelligent reflecting surface aided SWIPT," *IEEE Wireless Commun. Lett.*, Dec. 2019, doi: 10.1109/LWC.2019.2961656.
- [18] C. Pan, H. Ren, K. Wang, M. Elkashlan, A. Nallanathan, J. Wang, and L. Hanzo "Intelligent reflecting surface aided MIMO broadcasting for simultaneous wireless information and power transfer," *IEEE J. Sel. Area. Commun.*, 2020.

- [19] X. Yu, D. Xu, and R. Schober, "MISO wireless communication systems via intelligent reflecting surfaces," in *Proc. IEEE/CIC ICC*, Changchun, China, Aug. 2019, pp. 735740.
- [20] Z. Chu, W. Hao, P. Xiao, and J. Shi, "Intelligent reflect surface aided multi-antenna secure transmission," *IEEE Wireless Commun. Lett.*, vol. 9, no. 1, Jan. 2020.
- [21] C. Guo, Y. Cui, F. Yang, and L. Ding, "Outage probability analysis and minimization in intelligent reflecting surface-assisted MISO systems," *IEEE Commun. Lett.*, doi: 10.1109/LCOMM.2020.2975182, Feb. 2020.
- [22] B. Lyu, D. T. Hoang, S. Gong, and Z. Yang, "Intelligent reflecting surface assisted wireless powered communication networks," in *Proc. WCNC Workshops*, Seoul, South Korea, Apr. 2020, pp. 1-6.
- [23] Y. Zheng, S. Bi, Y. J. Zhang, Z. Quan, and H. Wang, "Intelligent reflecting surface enhanced user cooperation in wireless powered communication networks," *IEEE Wireless Commun. Lett.*, doi: 10.1109/LWC.2020.2974721, Feb. 2020.
- [24] C. Huang, G. C. Alexandropoulos, A. Zappone, M. Debbah, and C. Yuen, "Energy efficient multi-user MISO communication using low resolution large intelligent surfaces," in *Proc. IEEE GLOBECOM Workshops*, Abu Dhabi, United Arab Emirates, 2018, pp. 1-6.
- [25] C. Huang, A. Zappone, G. C. Alexandropoulos, M. Debbah, and C. Yuen, "Reconfigurable intelligent surfaces for energy efficiency in wireless communication," *IEEE Trans. Wireless Commun.*, vol. 18, no. 8, pp. 4157-4170, Jun. 2019.
- [26] Y. Zou, Y. Liu, S. Gong, W. Cheng, D. T. Hoang, and D. Niyato, "Joint energy beamforming and optimization for intelligent reflecting surface enhanced communications," in *Proc. WCNC Workshops*, Seoul, South Korea, Apr. 2020, pp. 1-6.
- [27] A. A. Nasir, X. Zhou, S. Durrani, and R. A. Kennedy, "Relaying protocols for wireless energy harvesting and information processing," *IEEE Trans. Wireless Commun.*, vol. 12, no. 7, pp. 3622-3636, Jul. 2013.
- [28] Z. Q. Luo, W.-K. Ma, A. M.-C. So, Y. Ye, and S. Zhang, "Semidefinite relaxation of quadratic optimization problems," *IEEE Signal Process.*, vol. 27, no. 3, pp. 20-34, May 2010.
- [29] S. Boyd and L. Vandenberghe, *Convex Optimization*. Cambridge University Press, 2004.
- [30] Michael Grant *et al.*, "CVX: Matlab software for disciplined convex programming," version 2.0 beta. <http://cvxr.com/cvx>, September 2013.
- [31] A. M.-C. So, J. Zhang, and Y. Ye, "On approximating complex quadratic optimization problems via semidefinite programming relaxations," *Mathematical Programming*, vol. 110, no. 1, pp. 93110, Jun. 2007.
- [32] V. Arun and H. Balakrishnan, "RFocus: Practical beamforming for small devices". Available Online: <https://arxiv.org/pdf/1912.07794.pdf>, May 2019.